Few-Body Modes of Binary Formation in Core Collapse

Ataru Tanikawa[a,b,c,*], Douglas C. Heggie[d], Piet Hut[e,f], Junichiro Makino[a,f]

[a] *RIKEN Advanced Institute for Computational Science, 7–1–26, Minatojima-minami-machi, Chuo-ku, Kobe, Hyogo, 650–0047, Japan*
[b] *Center for Computational Science, University of Tsukuba, 1–1–1, Tennodai, Tsukuba, Ibaraki 305–8577, Japan*
[c] *School of Computer Science and Engineering, University of Aizu, Tsuruga, Ikki-machi, Aizu-Wakamatsu, Fukushima, 965–8580, Japan*
[d] *School of Mathematics and Maxwell Institute for Mathematical Sciences, University of Edinburgh, King's Buildings, Edinburgh EH9 3JZ*
[e] *Institute for Advanced Study, Princeton, NJ 08540, USA*
[f] *Earth-Life Science Institute, Tokyo Institute of Technology, 2–12–1 Ookayama, Meguro, Tokyo 152-8551, Japan*

Abstract

At the moment of deepest core collapse, a star cluster core contains less than ten stars. This small number makes the traditional treatment of hard binary formation, assuming a homogeneous background density, suspect. In a previous paper, we have found that indeed the conventional wisdom of binary formation, based on three-body encounters, is incorrect. Here we refine that insight, by further dissecting the subsequent steps leading to hard binary formation. For this purpose, we add some analysis tools in order to make the study less subjective. We find that the conventional treatment does remain valid for direct three-body scattering, but fails for resonant three-body scattering. Especially democratic resonance scattering, which forms an important part of the analytical theory of three-body binary formation, takes too much space and time to be approximated as being isolated, in the context of a cluster core around core collapse. We conclude that, while three-body encounters can be analytically approximated as isolated, subsequent strong perturbations typically occur whenever those encounters give rise to democratic resonances. We present analytical estimates postdicting our numerical results. If we only had been a bit more clever, we could have predicted this qualitative behaviour.

*e-mail: ataru.tanikawa@riken.jp, TEL: +81-78-940-5865

Keywords: Stellar dynamics, Method: N-body simulation, globular clusters: general

1. Introduction

In our previous paper, Tanikawa et al. (2011), hereafter referred to as Paper I, we started to investigate in detail the formation mechanism of the first hard binary during core collapse of a dense star cluster. While many studies have appeared that have focused on the macroscopic aspects of core collapse, during the last fifty years, to the best of our knowledge our paper was the first one to address the microscopic aspects, including the actual reaction network of the stellar encounters that gave rise to the formation of a hard binary.

In that study, we encountered two surprising deviations from what had become accepted as the standard picture of binary formation in core collapse. First, in many cases more than three bodies are directly and simultaneously involved in the production of the first hard binary. Second, we concluded that the core at deepest collapse was smaller than expected before, typically containing half a dozen stars or less.

In contrast, in the standard picture developed in the nineteen eighties, it was first assumed that the formation of hard binaries was essentially a three-body process, whose rate could be estimated assuming the typical density and velocity dispersion in the core. Second, it was concluded that the core would bounce around the time its membership had dropped to a few dozen stars. In Paper I, we cited papers by Goodman (1984, 1987). An additional reference is Hut & Inagaki (1985), where analytical arguments were used to predict that three-body binary formation would reverse core collapse when the core shrank to contain of order 100 stars (80 in their section IVa, and 150 in their section IVbii). They also quoted simulations by McMillan & Lightman (1984) which showed core collapse to be reversed when the core contained 25 stars.

The two main flaws in the traditional picture are related. Given that the fluctuations in thermodynamic properties in a group of only a few stars are far larger than in a group of, say, thirty stars, the concept of a homogeneous temperature (or velocity dispersion) in the core is no longer valid for such a small core. Also, in a core containing only, say, five stars it is quite likely that all five are involved in the formation of a hard binary, with possibly some of

the stars just outside the core also making a strong presence felt during a pass through the core.

Encouraged by the fact that the standard story of hard binary formation needed to be corrected on at least these two quite fundamental points, we continued our investigation, focusing in on only one of the many runs reported in Paper I, in an attempt to get further to the bottom of what is actually happening during core collapse in microscopic detail. Not wanting to introduce any bias, we decided to simply take the very first case described in Paper I.

The central new technique, introduced in Paper I, was to plot all pairwise distances for all stars in the core, as a function of time, during a short period of time just before hard binary formation. Using this technique, and interpreting the results by eye, was only feasible given the very small number of stars in the core. Together with visual interactive inspection of the 3-D orbits of the stars in the core, our new technique allowed a determination of roughly how many stars were involved at each time during the successive stages leading to the formation of the first hard binary.

In this paper, we move beyond the detection of the new physics reported in Paper I, i.e. many-body binary formation, in order to perform a more detailed and quantitative analysis of this binary-formation process. In particular, we devote efforts to finding stars involved with the binary formation more objectively, and to reveal what kind of subsystems these stars construct, and how these stars and subsystems interact with each other. For this purpose, we introduce two other new techniques. The first one is the use of work functions, and the second one is a form of subcluster analysis. In addition, we have employed a better interactive visualisation tool, in the form of an `open-GL` program. These tools will be useful to make clear binary formation in more realistic and complicated N-body simulations in which stars have different masses and experience internal evolution.

In the process of applying these new tools, we again found new physics: while the main conclusions of Paper I hold, we now understand in more detail exactly why they hold. The main reason is the presence of democratic resonance interactions, a concept introduced by Hut (1982), which is a kind of encounter between a hard binary and a single intruder in which a third body is temporarily bound to the binary, in such a way that the subsequent motion cannot be described as a hierarchical triple system. In contrast, we found that the traditional perturbative treatment is in fact satisfactory for direct three-body interactions. It is only because democratic resonance

interactions last long and take up a large fraction of the space in the core that they will typically undergo strong encounters with other stars before a democratic resonance is finished.

This new paper has two main aims: first, to illustrate the new diagnostic tools and their uses (with a long-term goal of making this kind of analysis more streamlined and automatic), and, second, to explain our developed understanding of the new dynamical processes which we are exploring. This main finding is described in more detail in the discussion and conclusion sections below. The next two sections focus on a summary of what we found out about the first run in Paper I; and on what we learned in our new analysis in this paper, respectively. The section after that extends the analysis of Paper I to earlier times, where interesting processes were already happening that had not been flagged in Paper I. The paper finishes with a section of theoretical discussion, and then a summary of our conclusions and some outlook.

2. Summary of the first run in Paper I

The analysis in Paper I consisted mostly of inspection-by-eye, which sufficed to find the new physical phenomena, mainly the fact that more than three stars were involved in most instances of hard binary formation. Here follows a brief summary of the first run of Paper I, the 1024-body run with seed 1.

We performed an N-body simulation of a star cluster. At the initial time, it had 1024 stars with equal masses, and a stellar distribution given by the Plummer model. For the N-body simulation, we have used an N-body simulation code `GORILLA` (Tanikawa & Fukushige, 2009). In this simulation, the first binary is formed during the interval $18.323t_{\rm rh,i}$ – $18.442t_{\rm rh,i}$, where $t_{\rm rh,i}$ is the half-mass relaxation time at the initial time, and the half-mass relaxation time is defined by Spitzer & Hart (1971). We have defined the first binary as a binary whose binding energy is more than $10kT$, where $3/2kT$ is the average kinetic energy of cluster stars at the initial time. Additionally, this binary survives until it escapes from the cluster.

During the interval when the first binary is formed ($18.323t_{\rm rh,i} - 18.442t_{\rm rh,i}$), we take snapshots at every $0.01t_{\rm cr,c}$, where $t_{\rm cr,c}$ is instantaneous core crossing time. The instantaneous core crossing time is given by

$$t_{\rm cr,c} = \frac{r_{\rm c}}{v_{\rm c}}, \tag{1}$$

where r_c is the core radius defined by Casertano & Hut (1985) with modifications of McMillan et al. (1990), and v_c is the stellar velocity dispersion in the core. Using these snapshots, we have analysed orbits of stars involved in the first-binary formation. Here, we introduce τ, which is time scaled by the current $t_{cr,c}$, expressed as

$$\tau = \int \frac{dt}{t_{cr,c}}. \tag{2}$$

The time τ is useful for understanding dynamical processes in the core. We define $\tau = 0$ as the time when the first binary is formed. In terms of τ, we take the snapshots from $\tau = -67.93$ to $\tau = 76.17$. In order to reduce the data sizes of these snapshots, we include only subsets of stars in these snapshots. Generally we define these subsets as the stars in the core. If the number of stars in the core is less than 40, however, we include the 40 nearest stars around the density centre, which is also defined as in Casertano & Hut (1985), in these snapshots.

Figure 1 shows the time evolution of separations between stars involved in binary formation, in units of a_0, where a_0 is the semi-major axis of a binary with binding energy $1kT$. This figure is almost the same as fig. 7 of Paper I. In Paper I, we drew the orbits of only six stars numbered from 1 to 6. Here we have added two more stars, in order to highlight further some of the earlier stages of these interactions, around time $\tau = -4$. In Paper I, the six stars were chosen in the following way.

First, we followed the run from the beginning in order to find the first binary with a total energy of more than $10kT$, which turned out to be the binary (1,2) at $\tau = 0$. Next, we extended our search backwards in time, from that point on, to look for stars that had significant reactions with the final binary components, from $\tau = 0$ back to -1.6. We concluded that the hard binary came into being only at $\tau = -1.6$. In fact, binaries with energy less than $10kT$ are present before $\tau = -1.6$. For example, we can see in figure 2 that there is a binary with more than $9kT$ at around $\tau = -38$. However, we do not regard them as the first binary, since they disappear until $\tau = -4$. Although there are some pairs of stars with binding energy about $3kT$ during the interval $\tau = -4$ – -2, they should not be regarded as binaries. This is because their binding energies are strongly fluctuating. Typical binaries keep their binding energies constant, such as a binary with binding energy of $\sim 8kT$ during the interval $\tau = -37$ – -24.4.

Second, by considering the distances of other stars from 1 and 2, in the

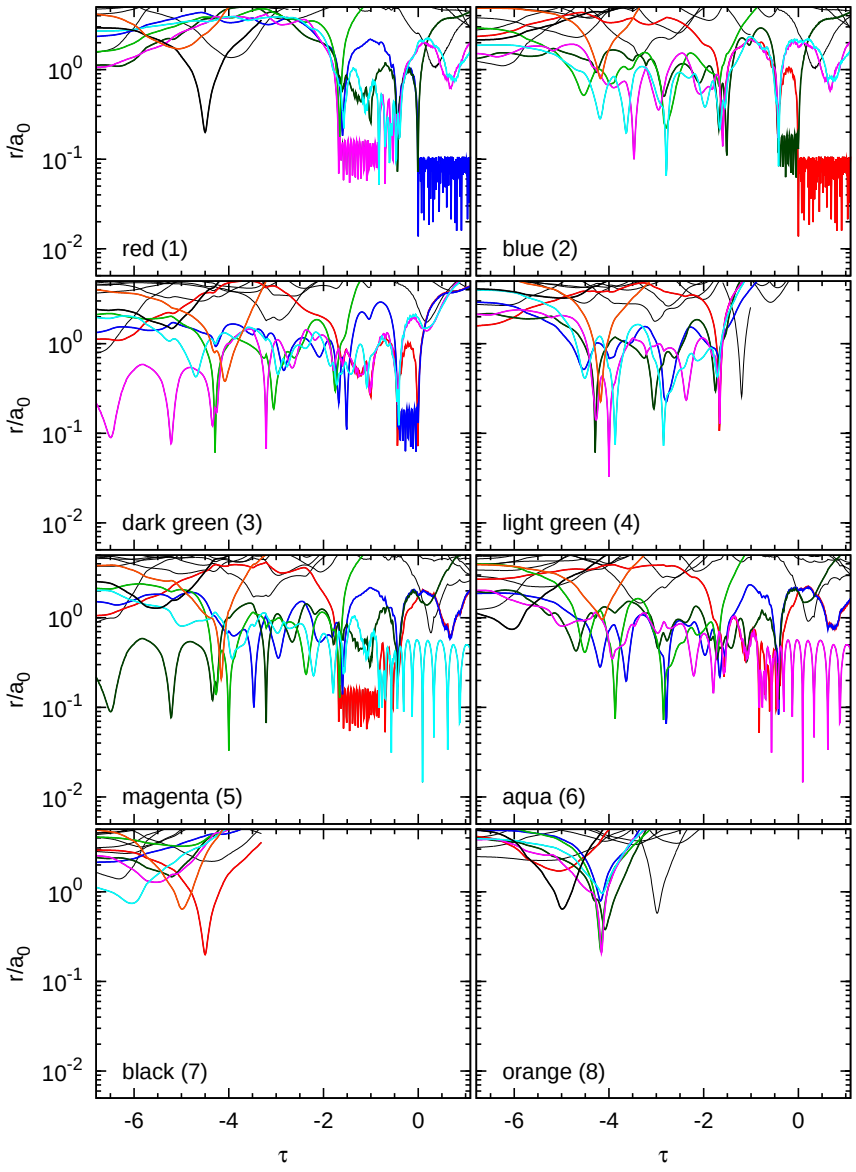

Figure 1: Time evolution of separations between stars involved in binary formation, which is almost the same as fig. 7 in Paper I, and is plotted over the same range of scaled time τ. This figure differs from Paper I, however, by the addition of stars 7 and 8, which are introduced in Sec.3.3. The definitions of τ and a_0 are in the main text.

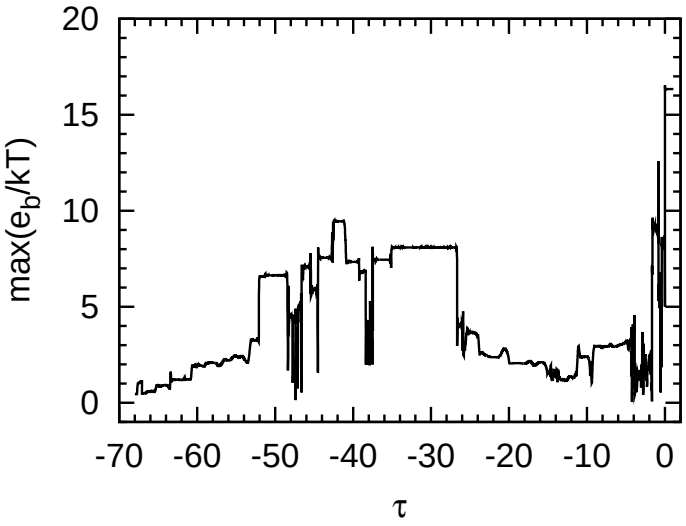

Figure 2: Time evolution of the maximum binding energy between any two stars (among the stars we followed) at each time.

top row of fig. 7 in Paper I (our figure 1), we found that stars 3 and 5 also played an important role: the presence of binaries (1,5) and (2,3) is obvious during the periods $-1.6 < \tau < -0.8$ and $-0.5 < \tau < 0$, respectively. In addition, star 4 makes a close encounter to star 1 at $\tau = -1.6$ in the top left panel (though the details are somewhat crowded) and star 6 can be seen to dance with stars 1 and 5 in the panels of the third row from $\tau = -0.8$ onwards.

Table 1: Dynamical interpretation of the first binary formation in Paper I and this paper.

Paper I		This paper	
τ	Events	τ	Events
$\lesssim -1.5$	interaction among stars 1, 2, 4, and 5 leads to formation of binary [1,5]	-1.6	interaction among stars 1, 2, 3, 4, 5, and 6 leads to formation of binary [1,5] ($9kT$)
$\gtrsim -1.0$	interaction among stars 1, 2, 3, 5, and 6 leads to dissolution of binary [1,5]	-0.8	invasion of star 6 into binary [1,5] leads to formation of democratic triple [1,5,6]
-0.5	formation of binary [2,3] from subsystem [1,2,3,5,6]	-0.5	invasion of stars 2 and 3 into democratic triple [1,5,6] leads to formation of binaries [2,3] and [5,6]
0.0	formation of binary [1,2] ($> 10kT$) by direct exchange	0.0	formation of binary [1,2] ($16kT$) by direct exchange

Table 1 summarises what can be gleaned from Paper I, in the left column. For comparison, we present in the right hand column somewhat refined information about these events as found in the current paper. Note that, in the "exchange" interactions in Table 1, a binary component is replaced by an intruder.

3. A new analysis of the first run of Paper I

3.1. Work Functions

In Paper I, we showed that more than three stars come close to each other at the first binary formation. However, we did not quantify how each star contributes to the binary formation. For this purpose, in the present paper we use binding energies and "work functions". The former and latter quantify binary formations and contribution of stars to the binary formations, respectively. Actually, the two quantities are useful not only for binary formation, but also for binary evolution, such as hardening, softening, and ionisation. Furthermore, we can generalise them to subsystems or multiple stars ("tuples" for short) which have more than two stars , so that a tuple with two stars is a binary.

The compactness of a tuple consisting of more than one star may be quantified by a binding energy. The binding energy of tuple i is expressed as

$$E_i(t) = \sum_{k<l}^{n_i} \frac{G m_{i_k} m_{i_l}}{|\boldsymbol{r}_{i_k} - \boldsymbol{r}_{i_l}|} - \frac{1}{2} \sum_{k}^{n_i} m_{i_k} \left(\boldsymbol{v}_{i_k}^2 - \boldsymbol{v}_{\rm cm}^2 \right), \tag{3}$$

where n_i is the number of components of tuple i, and $\boldsymbol{v}_{\rm cm}$ is the centre-of-mass velocity of tuple i, i.e. $\boldsymbol{v}_{\rm cm} = (\sum_k^{n_i} m_{i_k} \boldsymbol{v}_{i_k}) \,/\, (\sum_k^{n_i} m_{i_k})$. If the binding energy $E_i(t)$ is positive, tuple i is a bound system. We can extend this definition to a binding energy of a mixture of stars and subsystems. Then, we replace $m_{i,k}$, $\boldsymbol{r}_{i,k}$, and $\boldsymbol{v}_{i,k}$ in equation (3) by the mass and centre-of-mass position and velocity of a subsystem, respectively. In this way we can speak of the binding energy of a star to a subsystem of other stars, for example.

The binding energy allows us to identify bound subsystems that are temporarily almost unperturbed or isolated, as they have roughly constant binding energy. This raises the question of how these periods of roughly constant binding energy begin and end. Clearly, a significant amount of energy exchange between the subsystem and its surroundings is involved, at the beginning and the end of each such period. To characterise the energy exchange, we can look at the amount of work done during each event.

We start by determining the rate of energy exchange, defined as the amount of energy per unit time that the tuple i receives from a given star j:

$$\dot{E}_{i,j}(t) = -\sum_{k}^{n_i} \left[\boldsymbol{f}_{i_k,j} \cdot (\boldsymbol{v}_{i_k} - \boldsymbol{v}_{\rm cm}) \right], \tag{4}$$

where $\boldsymbol{f}_{i_k,j}$ is the force exerted by star j on component k of tuple i; this can be expressed as $\boldsymbol{f}_{i_k,j} = -Gm_j m_{i_k}(\boldsymbol{r}_{i_k} - \boldsymbol{r}_j)/|\boldsymbol{r}_{i_k} - \boldsymbol{r}_j|^3$. We call this quantity a "power function". Note, incidentally, that the "component" may itself be a subsystem, as before.

In order to find out which star or stars are responsible for a transition event we can compute the power function for various candidate stars j. But since the event is identified by means of the change in binding energy of tuple i, it is easier and more reliable to compare the *integral* of the power function with the binding energy of tuple i. We refer to this as a "work function". In practice we plot the graph of $E_i(t)$ along with the graphs of $E_{i,j}(t)$ for several candidate stars j. An example is the lower panel of figure 5, which will be discussed in Section 3.3.

3.2. Overview of the history for the binary formation

As we show in the remainder of this section, these diagnostics can be used to unravel the main interactions which eventually give rise to the first $10kT$ binary. On this basis it is possible to construct (manually) a schematic but detailed graphic description of these interactions (figure 3), in analogy with a diagram for a resonant three-body interaction presented by Hut & Bahcall (1983, fig.3). We sometimes refer to this as a kind of Feynman diagram, in analogy with somewhat similar figures used in perturbative quantum field theories. Though it depends on results which are still to be presented, it will aid the reader to follow the analysis with reference to this diagram.

In this reanalysis we divide the evolution into four phases: $-6.75 < \tau < -4.2$, $-4.2 < \tau < -1.6$, $-1.6 < \tau < 0.0$, and $0.0 < \tau < 1.1$. The start and end points merely delimit the range of times which were considered in detail in Paper I (see fig. 7 in Paper I, and figure 1 in the present paper). The other times are significant events identified in section 2 and table 1. These four phases are considered in the following sub-sections, and the phase before $\tau = -6.75$ is analysed in section 4.

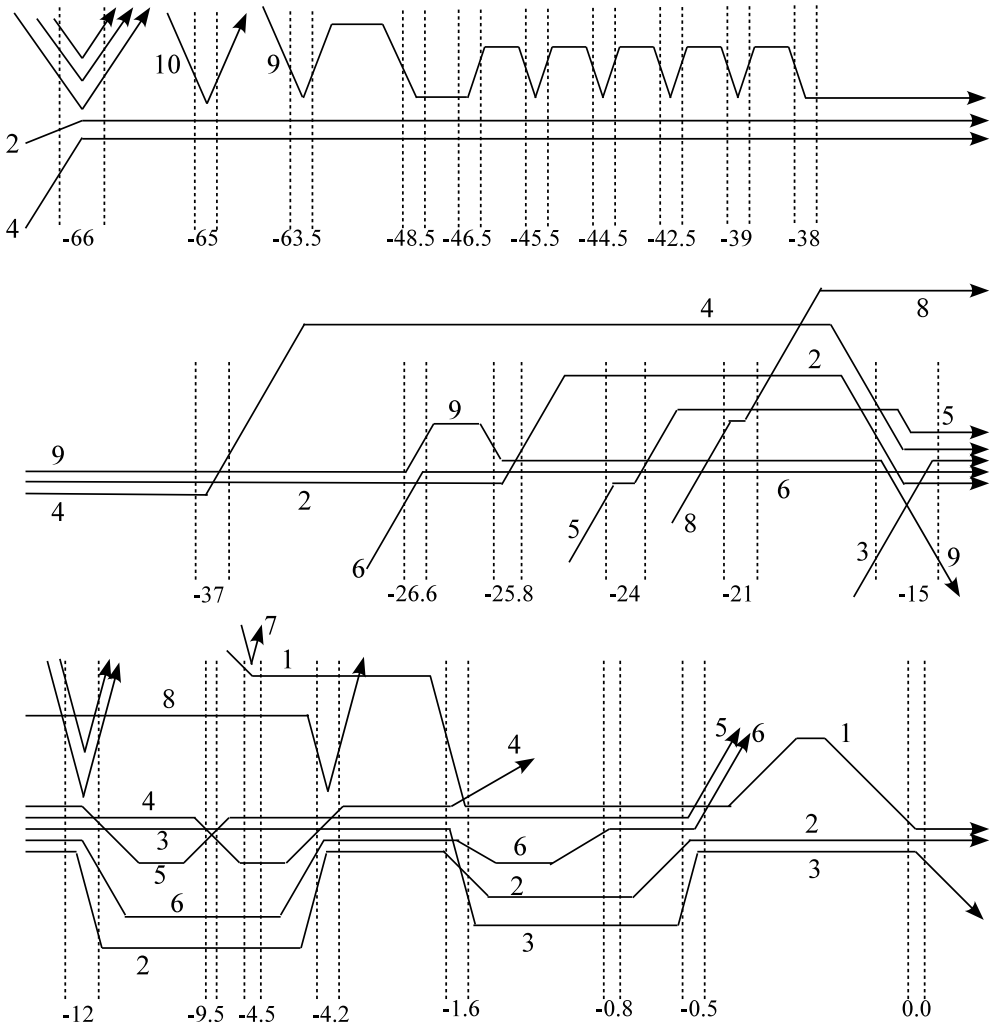

Figure 3: Illustration of interactions involved in the first binary formation. Close parallel lines indicate (schematically) temporary bound subsystems.

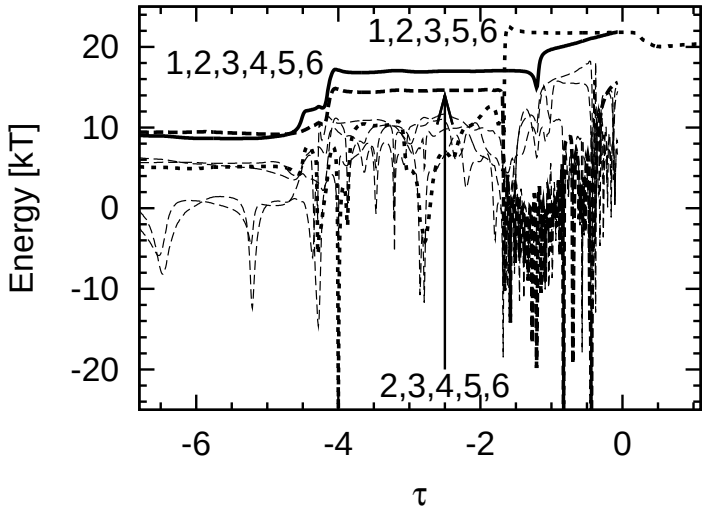

Figure 4: Time evolution of binding energies of the sextet (1,2,3,4,5,6) and any tuple of quintets in the sextet. Thick solid, dashed, and dotted curves indicate the binding energies of the sextet, the quintet (2,3,4,5,6), and the quintet (1,2,3,5,6), respectively, and thin dashed curves those of the other quintets.

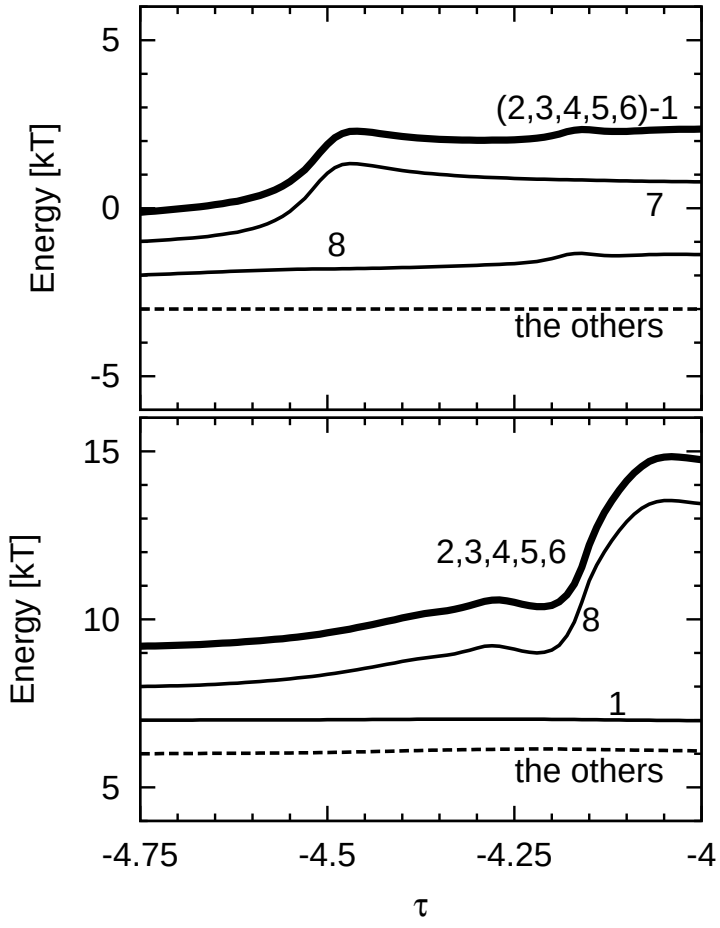

Figure 5: Time evolution of binding energies between a quintuple system (2,3,4,5,6) and star 1 (upper panel), and of the quintuple system (2,3,4,5,6) (lower panel), and of work done on them. The binding energies and work done are indicated by thick and thin curves, respectively. Numbers beside curves for the work indicate which stars do the work. The work is integrated from the time $\tau = -4.75$. In order to be eye-friendly, the initial values of the work done are not zero, which applies also for figures 9, 12, 15, 17, and 18.

3.3. The Era $-6.75 < \tau < -4.2$

Turning to the analysis of the first phase, $-6.75 < \tau < -4.2$, we see from the solid curve in figure 4 that system (1,2,3,4,5,6) is not isolated, as its binding energy changes abruptly at about $\tau = -4.5$ and $\tau = -4.2$. This is the reason why we include two additional stars in figure 1. At the former time, figure 1 (or fig. 7 in Paper I) shows a close approach to star 1 by a star which was unidentified in Paper I, but which we now label as star 7. In this encounter, the top panel of figure 5 shows that work is done by star 7 on a binary consisting of star 1 and the quintuple system (2,3,4,5,6). In this encounter, star 1 becomes bound to the quintuple system (2,3,4,5,6).

In the phase up to this event at $\tau = -4.5$, five stars of the sextet components (stars 2, 3, 4, 5, and 6) are bound with a binding energy of about $10kT$ (see the thick dashed curve in figure 4), and the five stars compose a quintuple system (2,3,4,5,6). Star 1 is unbound to the quintuple system, as can be seen in the top panel of figure 6. The quintuple system is unperturbed until the event at $\tau = -4.5$, since its binding energy is kept constant. Actually, three hitherto unnumbered stars are weakly bound to the quintuple system at $\tau = -6.75$, but they have gradually become unbound by $\tau = -5$ (see the middle panel of figure 7). They are not members of the quintuple system. We conclude that the quintuple system (2,3,4,5,6) is nearly isolated from the other stars during this phase up to $\tau = -4.5$, while star 1 is unbound to the quintuple system.

It is important to confirm that no other stars are involved in the binding of the system (2,3,4,5,6),1 at $\tau = -4.5$, and the hardening of the quintuple system (2,3,4,5,6) at $\tau = -4.2$. In both cases the work function by other stars included in snapshots, which we take in a way described in section 2, varies only a little (see dashed curves in both of the panels of figure 5).

Now we investigate the substructures of the quintuple system (2,3,4,5,6) described above. First, as seen in the top panel of figure 8, there is a binary (3,5) with about $3kT$, which corresponds to a pair of stars with binding energy $3kT$ during $\tau = -9.5$ – -4.2, seen in figure 2. The other three stars compose no binary. These three stars are not bound to each other as a democratic triple system (see the lowest solid black curve in the top panel of figure 8). Thus the quintuple system (2,3,4,5,6) consists of four components: one binary (3,5), and three single stars 2, 4, and 6. These four components are bound with energy $6kT$ (see the bottom panel of figure 8).

Next, we analyse how these four components are structured. We can see from the middle panel of figure 8 that pairs between the binary (3,5) and

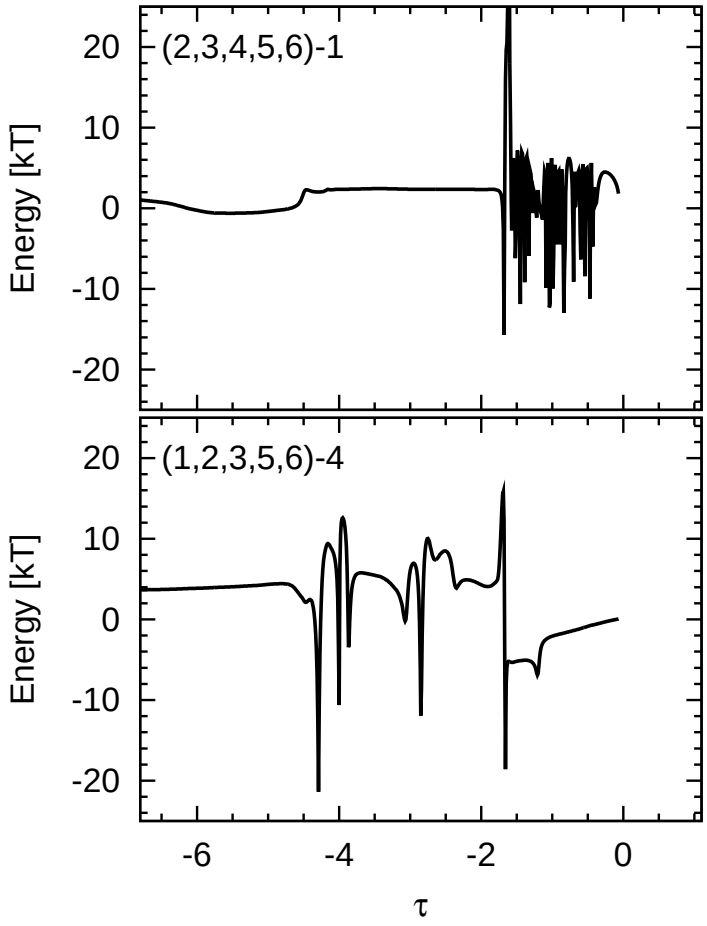

Figure 6: Time evolution of the binding energies between the quintet (2,3,4,5,6) and star 1 (top), and between the quintet (1,2,3,5,6) and star 4 (bottom).

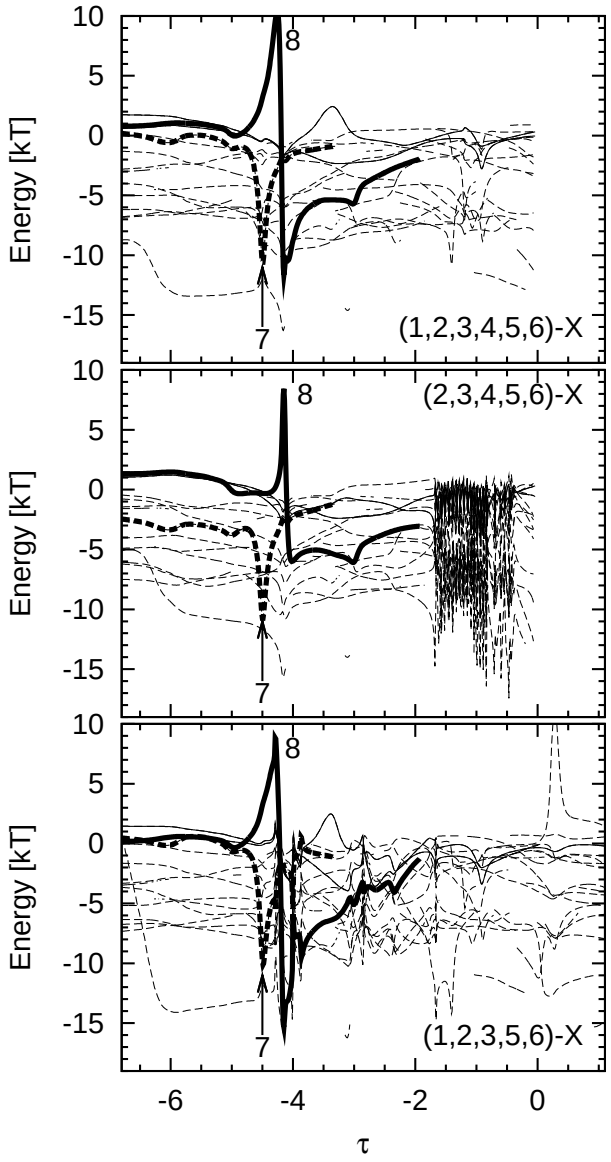

Figure 7: Time evolution of binding energies between a star "X" and either the sextet (1,2,3,4,5,6) (top) or one of the quintets (2,3,4,5,6) (middle) and (1,2,3,5,6) (bottom). The star "X" is usually unnumbered. Two stars which are particularly bound to the sextet (or quintet (2,3,4,5,6)) are indicated by solid curves: the star 8 is shown by a thick solid curve, and star 7 by a thick dashed curve; the other stars are shown by thin dashed curves. The distances of the stars 7 and 8 are shown in figure 1.

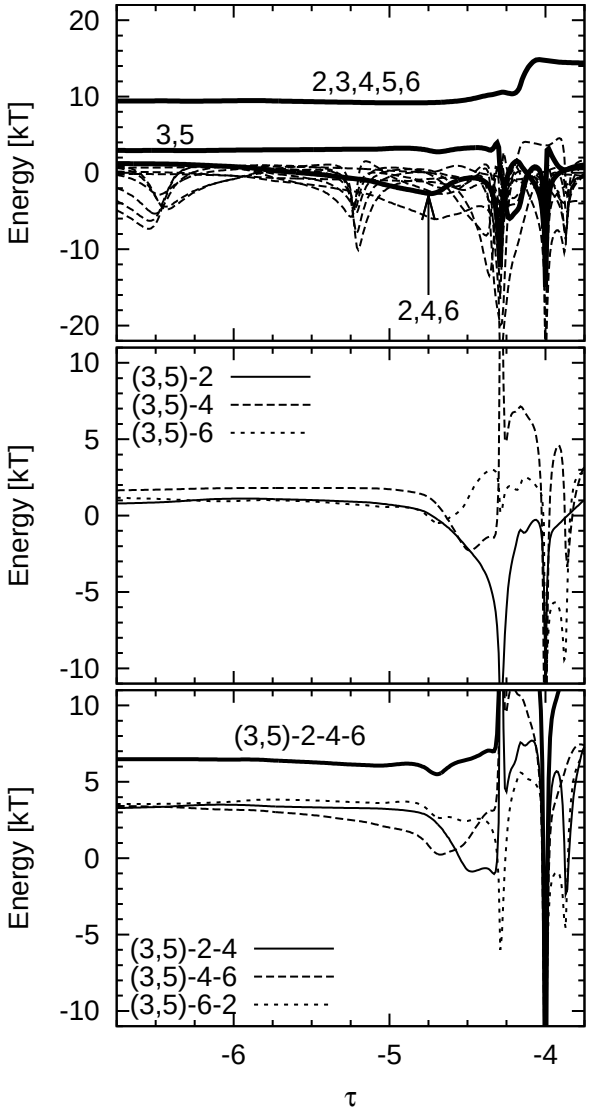

Figure 8: (Top) Time evolution of binding energies among a quintet (2,3,4,5,6) and a trio (2,4,6), and between any pair in the quintet. Thick curves show the binding energies among the quintet and the trio, and between a pair (3,5), and dashed curves those between all the pairs, except the pair (3,5). (Middle) Time evolution of binding energies between the pair (3,5) and either one of stars 2, 4, and 6. (Bottom) Time evolution of binding energies among the binary (3,5) and all of stars 2, 4, and 6, and among the binary (3,5) and any two of the stars 2, 4, and 6.

either of the other three stars have positive binding energies, and that their binding energies are kept almost constant. This means that the binary (3,5) and the other three stars compose hierarchical triple systems individually, and that they are not perturbed much by each other.

The binary (3,5) plays an important role in binding the four components which are obtained by choosing any three of the four objects (3,5), 2, 4 and 6. Three of these four components have positive binding energies, i.e. the three which include the binary (3,5) (see the bottom panel of figure 8). On the other hand, the three single stars are unbound (see the top panel of figure 8). Therefore, the configuration of these four components is not democratic, but similar to a planetary system; the binary and single stars correspond to a sun and planets, respectively.

In summary, the quintuple system (2,3,4,5,6) has four components: a binary (3,5) and three single stars, in a configuration analogous to a planetary system. This configuration breaks down soon, however, since the mass ratios of the binary to the single stars are not large. In fact the binary (3,5) is ionised at the end of the current phase. This binary is destroyed by star 4. As seen in figure 9, star 4 does work on the binary (3,5) at the moment when its binding energy becomes negative. No other stars do work on the binary (3,5).

Now we describe the other events around the close of the phase, i.e. $\tau = -4.2$. At this time the binding energies among the sextuple component (1,2,3,4,5,6) and among the quintet component (2,3,4,5,6) become larger (see figure 4), while the binding energy between the quintuple system (2,3,4,5,6) and star 1 is kept almost constant (see the top panel of figure 6). This means that the quintuple system (2,3,4,5,6) becomes bound more tightly. This event results from work done by a hitherto unnamed star which we subsequently refer to as star 8, and which intrudes into the quintuple system (2,3,4,5,6) at the time of the event (see figure 1). From the bottom panel of figure 5, we see that star 8 is almost entirely responsible for the increase in binding energy of the quintuple around $\tau = -4.2$. At the same time star 8 slightly hardens the binary consisting of star 1 and the quintuple system (2,3,4,5,6) (see the top panel of figure 5). However, its effect is small, compared to that of star 7 a short time earlier.

3.4. The Era $-4.2 < \tau < -1.6$

As we have seen, by the start of the second phase, star 1 has joined the quintuple system (2,3,4,5,6). Throughout the second phase the binding

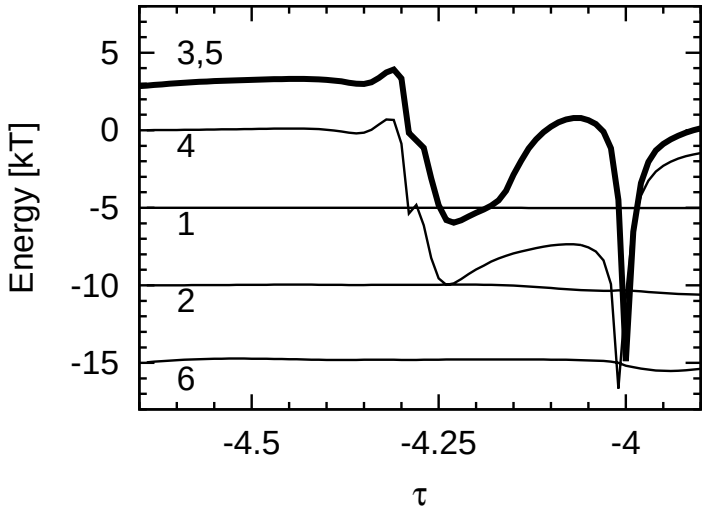

Figure 9: Time evolution of the binding energy of the binary (3,5) (thick curve), and work done by the four numbered stars 1, 2, 4, and 6 on this binary (thin curves). Numbers beside the work curves indicate the relevant star. The work is integrated from the time $\tau = -4.65$.

energy between star 1 and the quintuple system is positive, about $2kT$, and constant (see the top panel of figure 6). The sextet (1,2,3,4,5,6) forms a bound sextuple system, and is unperturbed by other stars (figure 4). Indeed no other star is continuously bound to this sextuple system (see the top panel of figure 7). Since the binding energy of the quintuple system (2,3,4,5,6) is also constant (see figure 4), the quintuple system is unperturbed by other stars including star 1, as star 1 is far from the other numbered stars (see figure 1). In practice, the quintuple system (2,3,4,5,6) survives undisturbed from the previous phase.

In order to investigate the internal structure of the quintuple system, we focus on all the tuples consisting of its components. After the soft binary (3,5) is destroyed at $\tau \sim -4.25$, no persistent substructure is formed until the end of this phase, at $\tau = -1.6$. As seen in all the panels of figure 10, no binding energy of any tuple keeps constant during this phase. Occasionally, the binding energies of some tuples are temporarily positive. However, their lifetime is less than unity in the units of τ, which is similar to the crossing time of the quintuple system (2,3,4,5,6). We conclude that the quintuple system has a democratic configuration, and therefore we can write the configuration of the sextuple system as [(2,3,4,5,6),1]. This is consistent with the conclusion, described in section 2, that the hard binary came into being only at $\tau = -1.6$.

At $\tau \sim -1.6$, the end of the second phase, or the beginning of the third phase, the sextuple system (1,2,3,4,5,6) changes dramatically. Star 1 intrudes into the quintuple system (2,3,4,5,6), an interaction which results in the ejection of star 4 from the sextuple system (1,2,3,4,5,6). During this interaction, the sextet (1,2,3,4,5,6), which is bound before $\tau = -1.6$, is unperturbed by the other cluster stars, since the binding energy among the sextet components is constant before and (for a short time) after this interaction (see figure 4). On the other hand, star 4 becomes unbound to the new quintuple system (1,2,3,5,6): the binding energy between star 4 and the new quintuple system becomes and remains essentially negative (see the bottom panel of figure 6). From the right second-row panel of figure 1, we can also see that star 4 recedes from all the components of the new quintuple system.

3.5. The Era $-1.6 < \tau < -0.8$

In this section, we focus on the quintuple system (1,2,3,5,6) and its internal structure. In the third phase $-1.6 < \tau < -0.8$, and indeed throughout the interval $-1.6 < \tau < 0.0$, the new quintet members (1,2,3,5,6) are bound

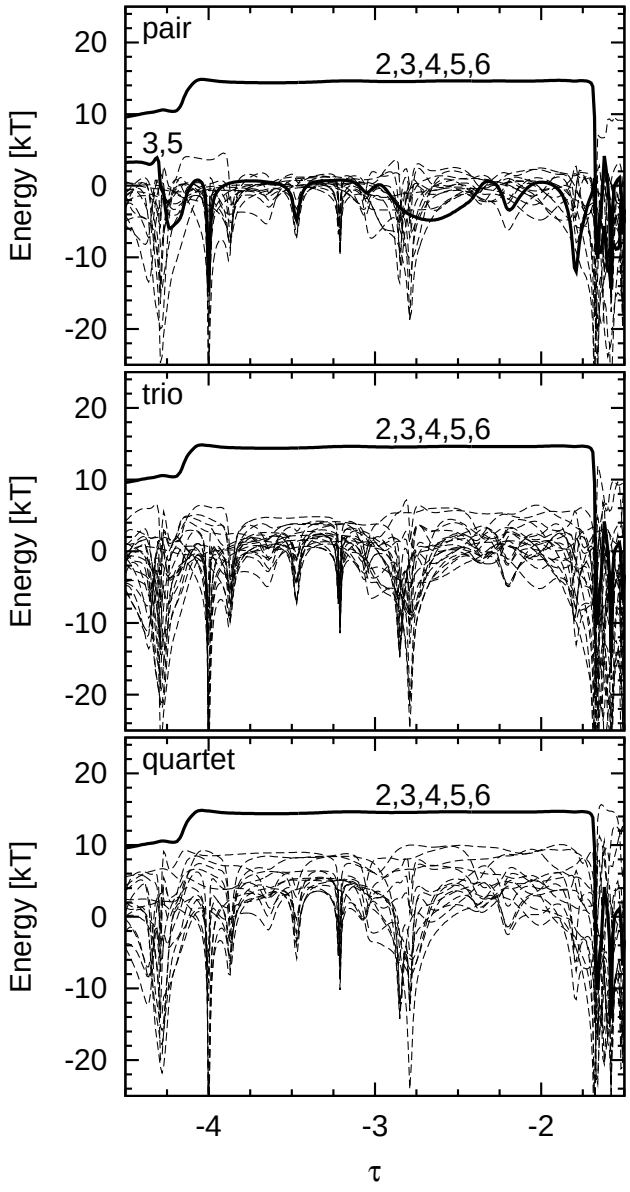

Figure 10: Time evolution of binding energies of a quintet (2,3,4,5,6) (each panel) and any pair (top), any trio (middle), and any quartet (bottom) in the quintet. All these pairs, trios, and quartets are indicated by dashed curves, except the pair (3,5) (solid curve).

to each other. In fact the binding energy of the quintuple system is more than $20kT$, as can be seen in figure 4. It is almost isolated, since its binding energy keeps constant during this phase. No other star is continuously bound to this quintuple system (see the bottom panel of figure 7). Star 4 was ejected from the sextet (1,2,3,4,5,6) in the creation of the new quintet, and it can be seen in the lower panel of figure 6 that the binding energy between star 4 and the quintuple system is perturbed by an event at $\tau = -1.25$. This is caused by an encounter with an unnamed star (figure 1), which also affects the binding energy of the sextet (figure 4).

First, we search for substructures which consist of binary stars. There is only one, a binary (1,5) with energy $9kT$ (see the top panel of figure 11), and the other three stars do not compose any binary or triple system (see the top panel of figure 11). Next, we seek stable substructures which contain the binary (1,5) and single stars 2, 3, and 6. We can see from the middle panel of figure 11 that the binding energy among the binary (1,5) and two single stars 3 and 6 remains constant during $-1.5 < \tau < -0.8$. This means that the quadruple system (1,3,5,6) is unperturbed by star 2. This quadruple system is bound to star 2, and the pair consisting of this quadruple system and star 2 is unperturbed by the other stars (see the bottom panel of figure 11).

Now we focus attention on the internal structure of the quadruple system (1,3,5,6) containing the binary (1,5) and two single stars 3 and 6. The binding energy of pair (3,6) is negative (see the top panel of figure 11), and those between the binary (1,5) and either one of stars 3 and 6 are positive (see the middle panel of figure 11). This means that they compose a planetary system ; the binary (1,5) is a sun and stars 3 and 6 are planets, similarly to the quintuple system (2,3,4,5,6) during $\tau < -4.2$. However, the binding energies between the binary (1,5) and either one of stars 3 and 6 are fluctuating, and therefore the "planets" perturb each other.

In summary, the structure of the quintuple system (1,2,3,5,6) may be summarised as {[(1,5),3,6],2}. Note that the quadruple system (1,3,5,6) is structured as a sort of planetary systems in which the binary (1,5) is a sun, and stars 3 and 6 are planets; they are *not*, however, a democratic triple system with respect to the binary (1,5) and single stars 3 and 6.

We now consider the formation of the new substructures which originated near the start of this phase, i.e. the binary (1,5) and the quadruple system (1,3,5,6). The top panel of figure 12 shows the evolution of the binding energy of the binary (1,5) and the work done by stars 2, 3, 4, and 6 on this

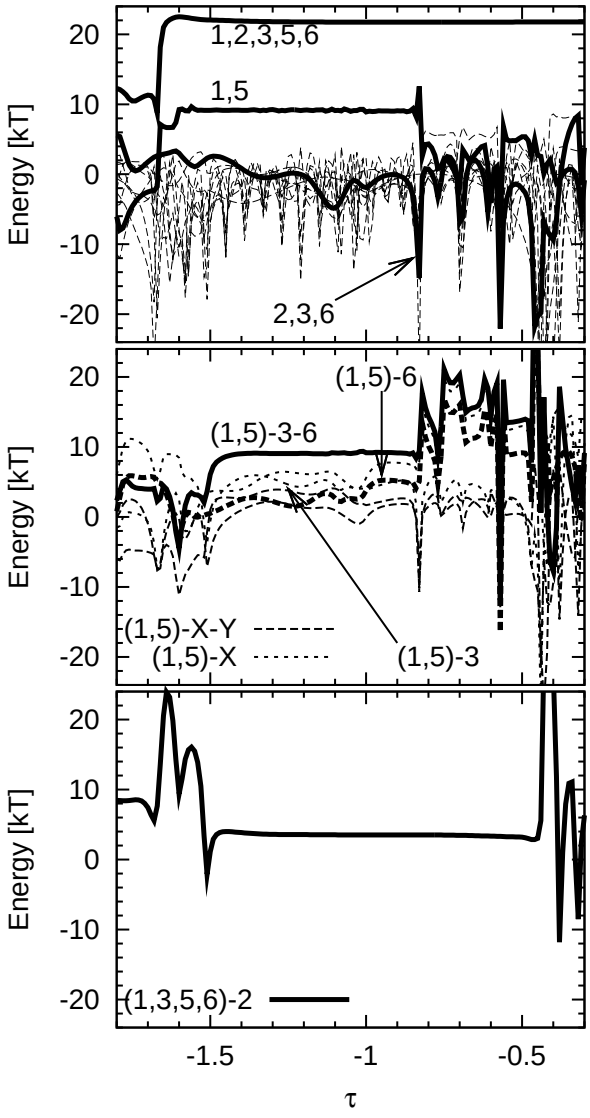

Figure 11: (Top) Time evolution of binding energies between any pair of components in the quintet (1,2,3,5,6), and among the trio (2,3,6). Dashed curves indicate binding energies between all the pairs, except the pair (1,5). (Middle) Time evolution of binding energies between the pair (1,5) and any one of the stars 2, 3, and 6, and among the pair (1,5) and any two of the stars 2, 3, and 6. (Bottom) Time evolution of binding energies between the quartet (1,3,5,6) and star 2.

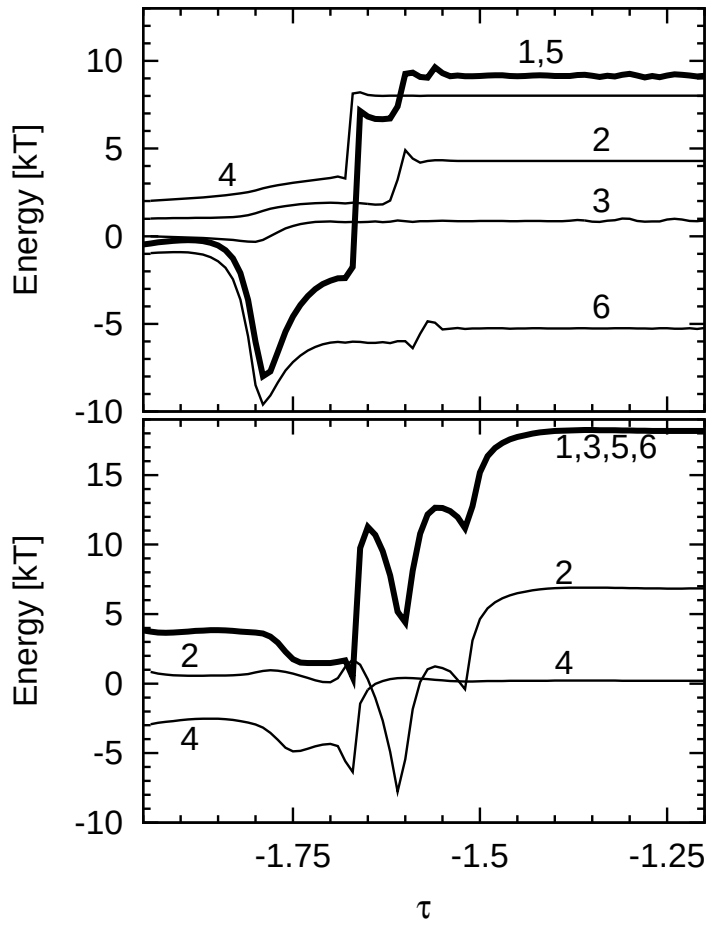

Figure 12: Time evolution of the binding energies of a binary (1,5) and a quadruple system (1,3,5,6), and of work done on these substructures by the corresponding numbered star. The work is integrated from the time $\tau = -1.95$.

binary. We do not need to consider the work done by the other stars; the sextuple system (1,2,3,4,5,6) is isolated during this phase, which can be seen in the constancy of the binding energy of the sextuple system (1,2,3,4,5,6) throughout the current phase (see figure 4).

As seen in the top panel of figure 12, the binding energy of the binary (1,5) is mainly increased by work done by star 4. Stars 2 and 6 also contribute to the increase of its binding energy after the binary (1,5) has become hard ($\sim 8kT$). However, they perturb the binary (1,5) only marginally. We also see the binding energy of the quadruple system (1,3,5,6) plotted in the bottom panel of figure 12. We can say that the quadruple system is formed and hardened by work done by star 4 at $\tau = -1.65$, and by work done by star 2 at $\tau = -1.5$, two events which help to isolate the quadruple from external disturbance.

3.6. The Era $-0.8 < \tau < -0.5$

In this phase, the quintuple system (1,2,3,5,6) survives without external disturbance from the previous phase (see the top panel of figure 11). However, its internal structure is changed.

First we consider substructures consisting only of two or three stars. There is no persistent binary in the quintuple system (see the top panel of figure 11), but there is a triple system (1,5,6) (see the top panel of figure 13). This triple system is democratic, since no pair in this triple system is bound by themselves (see the top panel of figure 11 again).

The democratic triple system (1,5,6) is bound to both stars 2 and 3. The pair between the triple system and star 3 is unperturbed by the other stars (see the bottom panel of figure 13). On the other hand, the pair between the triple system and star 2 is slightly perturbed: note that the binding energy of the pair continues to increase slowly throughout this phase (see the bottom panel of figure 13). This pair may be perturbed by star 3, since the separation between the triple system and star 2 is larger than that between the triple system and star 3; this can be seen with a little difficulty in figure 1, and also from the fact that star 3 is more tightly bound to the triple than star 2 is (the lower panel of figure 13). The assumption that no external star is involved is supported by the bottom panel of figure 11, which shows that the quadruple (1,3,5,6) and star 2 are bound to each other and unperturbed. In summary, this discussion shows that the structure of the quintuple system may be written as {[(1,5,6),3],2}.

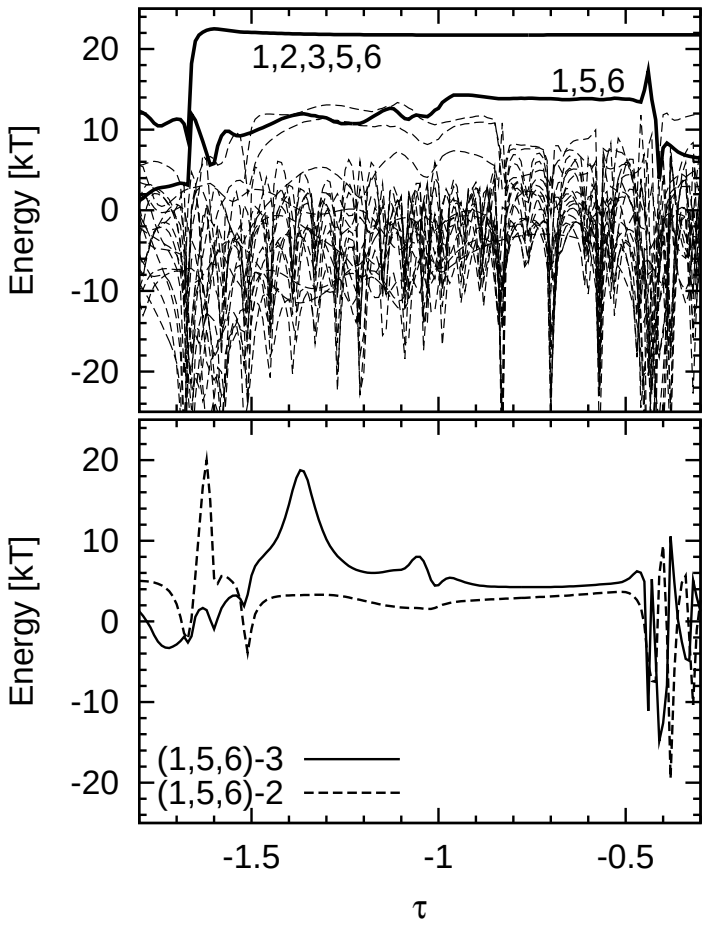

Figure 13: (Top) Time evolution of binding energies of a quintet (1,2,3,5,6) (a solid curve) and any trio in this quintet. The trio (1,5,6) is indicated by a solid curve, and the other trios by dashed curves. (Bottom) Time evolution of binding energies between the trio (1,5,6) and either one of stars 2 and 3.

The start of the present phase is marked by the disruption of binary (1,5), as can be seen in the top panel of figure 11. It is clear that this event is caused by the invasion of star 6 into the binary (1,5) , and results in the formation of the democratic triple system (1,5,6). We do not show the work function of star 6 for the binary (1,5), but the close interaction of these three stars at $\tau = -0.8$ is obvious enough in figure 1. From the point of view of our theoretical understanding, this is one of the most significant events in the entire evolution (see section 5.1).

3.7. The Era $-0.5 < \tau < 0.0$

In this phase, which strictly begins nearer $\tau = -0.4$, the quintuple system (1,2,3,5,6) persists from the previous phase, without perturbation by the other stars (see its binding energy in the top panel of figure 14). However, the internal structure is greatly changed. As seen in the top panel of figure 14, a hard binary (2,3) and soft binary (5,6) are formed. Their binding energies are, respectively, $8kT$ and $3kT$. Therefore, the five stars compose three components containing less than three stars each: the hard binary (2,3), soft binary (5,6), and a single star 1.

We now investigate binding energies between each pair of the above three components (see the middle panel of figure 14). We observe first that the binding energy between the binary (2,3) and star 1 is almost constant; in other words, they have a hierarchical configuration. The hierarchical triple system [(2,3),1] and the soft binary (5,6) are bound to each other (see also the middle panel of figure 14). We can abbreviate the structure of the quintuple system (1,2,3,5,6) as {[(2,3),1],(5,6)}.

Now we describe how the structure of the previous phase is transformed into the new structure, i.e. the transformation from {[(1,5,6),3],2} into {[(2,3),1],(5,6)}. We have to consider in particular the destruction and formation of the innermost structures: the destruction of the democratic triple system (1,5,6), and the formation of the hard binary (2,3) and the soft binary (5,6).

The democratic triple system is destroyed equally by both stars 2 and 3, which were its companions in the previous phase (see the top panel of figure 15). The triple also does work on stars 2 and 3, causing them to form a hard binary. In fact the work which forms this binary is mainly done by star 6, and marginally by star 1 (see the middle panel of figure 15).

Finally, we investigate the formation of the soft binary (5,6). As seen in the bottom panel of figure 15, the work of stars 1, 2 and 3 on the soft binary

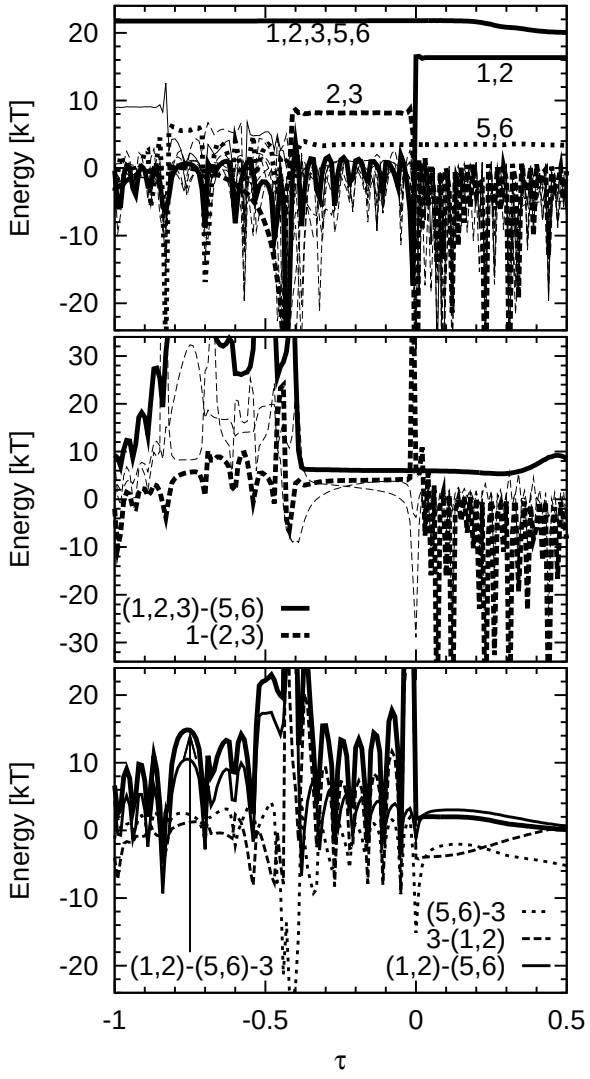

Figure 14: Time evolution of the quintuple system (1,2,3,5,6) and its substructure. (Top) Binding energy between any pair is shown: pairs (1,2) (thick solid curve), (2,3) (thick dashed curve), (5,6) (thick dotted curve), and the others (thin dashed curves). (Middle) Binding energies between any pair of three components: pairs (2,3) and (5,6), and star 1, and that between the trio (1,2,3) and the pair (5,6). The pairs of the two binaries (2,3) and (5,6) and of the binary (5,6) and star 1 are indicated by thin dashed curves. (Bottom) Binding energy among three components: pairs (1,2) and (5,6) and star 3, and those between any pair of the three components.

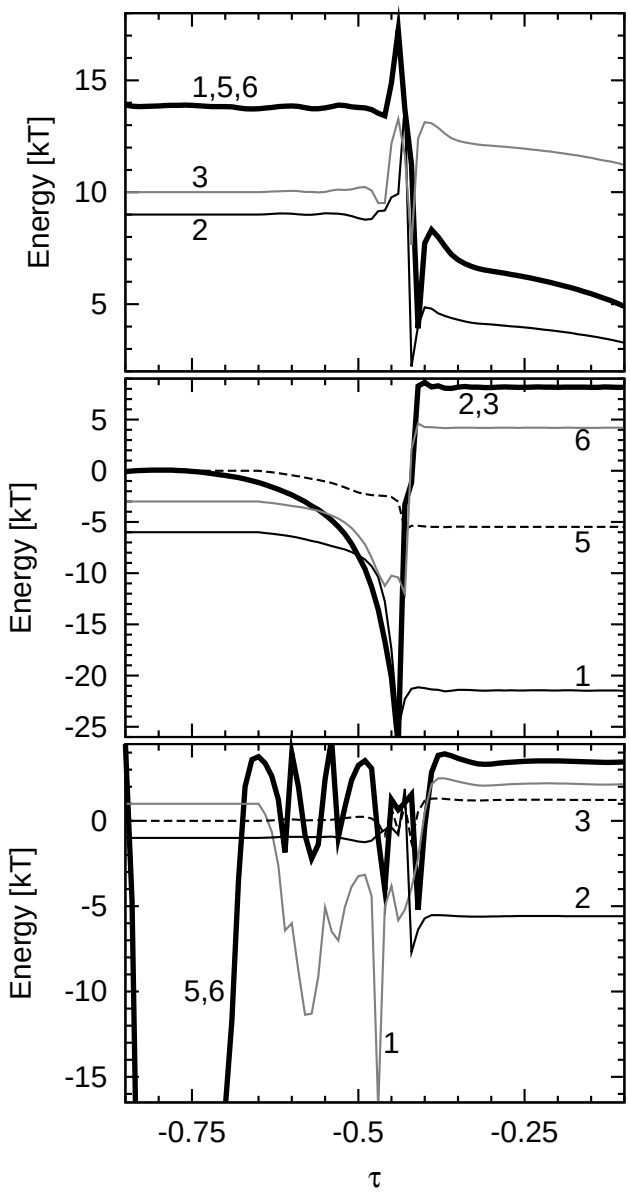

Figure 15: Time evolution of the binding energies of the trio (1,5,6) and pairs (2,3) and (5,6), and of work done on these substructures by the star identified by the label numbers. The work is integrated from the time $\tau = -0.65$.

(5,6) is complicated. However, it is clear that the work of star 1 contributes strongly to the binding of the soft binary (5,6). After the work done by star 1, the binding energy of the two stars 5 and 6 becomes positive. Note that a binary becomes more bound, i.e. has larger binding energy, if a given star works on the binary. The definitions of a binary's binding energy and work function can be seen in equations (3) and (4), respectively.

3.8. The Era $\tau > 0.0$

In the final phase, the structure becomes simple. As can be seen in the top panel of figure 14, there is one hard binary (1,2) with binding energy $16kT$, and one soft binary (5,6). The formation of the harder binary was the event which determined the origin of scaled time τ in Paper I. The soft binary lives from the previous phase. Thus the quintet (1,2,3,5,6) has three components: two binaries (1,2) and (5,6) and one single star 3. These three components eventually become unbound from each other. As can be seen in the bottom panel of figure 14, the binding energies between star 3 and either one of the binaries (1,2) and (5,6) are negative. The two binaries are bound at the beginning of this phase, but their binding energy reaches zero at time $\tau = 0.5$. The binding energy among the three components behaves in the same way as that between the two binaries (1,2) and (5,6). Indeed, in the phase $\tau > 0$, the binding energy of the quintuple system (1,2,3,5,6) itself begins to change (see the top panel of figure 14). As we shall see, the quintuple system is destroyed due to interactions among its components themselves at $\tau = 0$, and gradually the quintuple system becomes more easily perturbed by other stars.

In summary, the hard binary (1,2), the soft binary (5,6) and a single star 3 are left. They are unbound. This can be indicated by writing it as (1,2), (5,6), 3.

In the transition from the previous phase to the current one, at $\tau = 0.0$, the internal structure is changed from {[(2,3),1],(5,6)} to three unbound components, which are two binaries (1,2) and (5,6) and one single star 3. This takes place in the following way. Star 3 is replaced by star 1. This exchange interaction exerts a kick on star 3 and the new binary (1,2). This kick unbinds the three components. Since it is clear how the quintuple system is destroyed, we do not investigate these interactions in any more detail.

4. The prehistory of the first run of Paper I

Section 3 began just before the preexisting binary (3,5) is destroyed, and the first binary (1,2) emerges from the subsystem (1,2,3,4,5,6). What we show in the present section is that the history of these stars extends much further back. In particular, in order to investigate how the subsystem (1,2,3,4,5,6) and its binary (3,5) were formed, we now follow the orbits of the subsystem components and its surroundings before $\tau = -6.75$. We shall, however, confine the discussion to a presentation of results, and will generally not describe the use of binding energies and work functions on which the interpretation depends.

Figure 2 gives an overview of binary activity over a long period culminating with the formation of the $10kT$ binary (1,2) at $\tau = 0$. It shows the time evolution of the maximum binding energy between any pair of stars at each time. Before $\tau = -6.75$, at least one hard binary, which consists of stars 2 and 4, is formed, and its binding energy reaches $9kT$ at $\tau = -43$ (figure 2). The binary (2,4) persists for a while, exchanging its components with intruders several times. The binary consists of stars 6 and 9 at $\tau = -25.8$. However, the binary (6,9) is much softer than the original binary (2,4). By $\tau = -12$, there is no longer any binary with more than $2kT$. Curiously, the components of the binary at $\tau = -43$ belong to the subsystem whose evolution we followed in Section 3, and one of them is also a member of the "final" binary.

Now we check the formation and destruction processes of the $9kT$ binary in detail. Figure 16 shows the distances between the stars composing the subsystem mentioned in section 3. However, star 7, which has no role in the prehistory, is replaced with star 9.

We can see immediately that the $9kT$ binary consists of stars 2 and 4. By analysis analogous to that of Section 3, it is found that this binary is gradually hardened by encounters with several distinct stars, including star 9, from $\tau = -66$ to $\tau = -52$. At $\tau = -48.5$, star 9 intrudes into the binary. The binary and star 9 become a hierarchical triple system, which survives until $\tau = -38$. At $\tau = -37$, star 4 is exchanged with star 9, and a binary (2,9) is formed. The binary (2,9) is almost unperturbed for a long time, until $\tau = -26.6$.

At $\tau = -26.6$, star 6 falls into the binary (2,9), and the three stars 2, 6, and 9 form a temporary bound triple with a single ejection of star 9 which returns at $\tau = -25.8$. The temporary bound triple system ends up with the

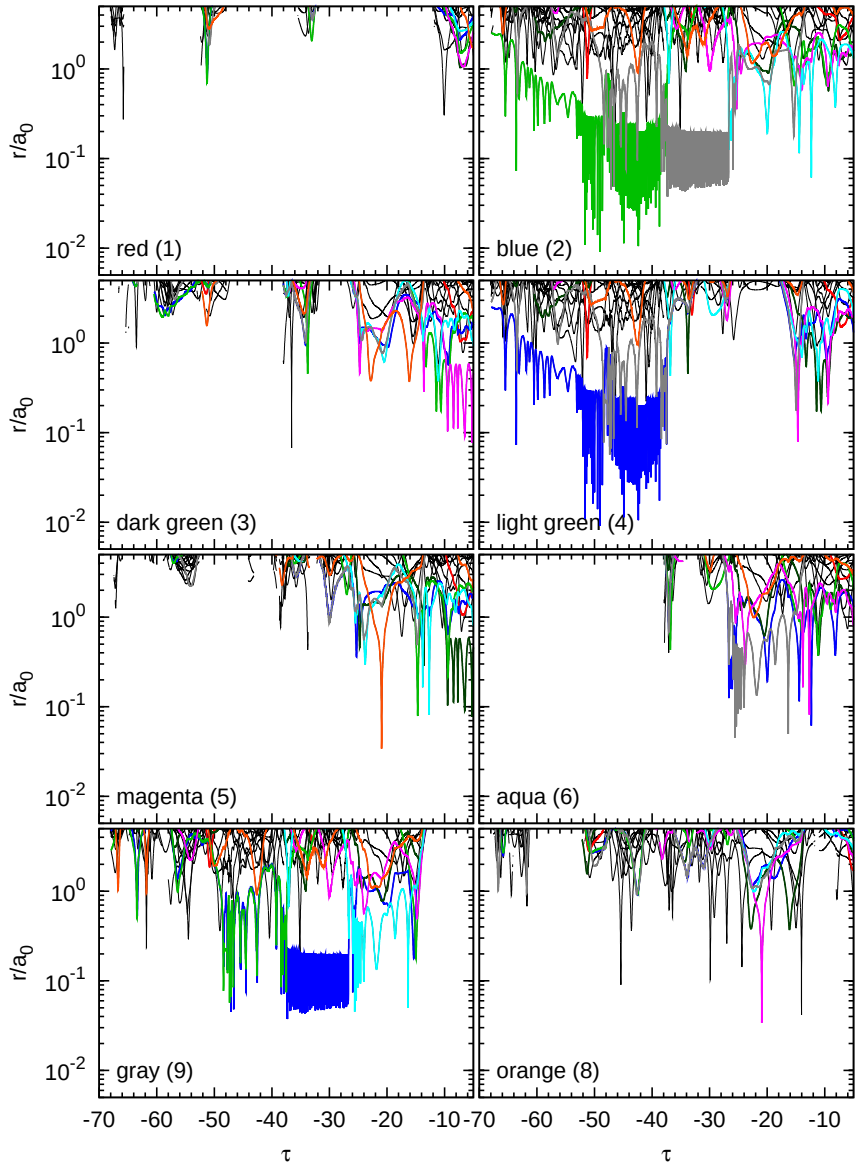

Figure 16: The same as figure 1, except that star 7 is replaced with star 9, shown in grey.

ejection of star 2, and the binary (6,9) is formed. The binary (6,9) is only half as hard as its progenitor binary (2,9) (as can just be seen in figure 2). The binary (6,9) is perturbed by stars 5 ($\tau = -24$) and 8 ($\tau = -21$), and finally destroyed by intrusions of stars 2, 3, 4, and 5 at $\tau = -15$. We return to this event at the end of this section.

After that, there is no binary until a binary (3,4) appears at $\tau = -12$. The binary component 4 is exchanged with star 5 at $\tau = -9.5$. The binary (3,5) is the same as a binary which we see from $\tau = -6.75$ to -4.2 in figure 1. It was with that binary that our discussion of the history began, in Section 3.3.

In the prehistory, two binaries are formed not by exchange interactions but by encounters involving more than three stars, i.e. binaries (2,4) at $\tau = -66$, and (3,4) at $\tau = -12$. We analyse their formation using work functions. Figure 17 shows the time evolution of the binding energy of the binary (2,4), and work functions for the binary. The binary (2,4) becomes harder in three phases from $\tau = -66$ to -63.5. Its hardening involves five stars: one set of three stars, which we do not identify otherwise, and successively stars 10 and 9. Similarly we can see from figure 18 that the binary (3,4) is formed and hardened through encounters with stars 5 and 6, though it is also hardened by two other (unnumbered) stars. Although star 2 is a member of the subsystem (2,3,4,5,6) existing at this time, star 2 does not contribute to the formation of the binary (3,4).

Finally, we focus on the formation of the subsystem (2,3,4,5,6) at $\tau = -15$. Star 6 is a component of the preexisting binary (6,9). Stars 2, 3, 4, and 5 dissolve the binary (6,9) around $\tau = -15$, and share out the binding energy of the binary (6,9). Ejection of star 9 also contributes to the binding energy of the subsystem (2,3,4,5,6).

5. Discussion

Paper I established a new framework for understanding the formation of the first long-lived binary in an equal-mass N-body system at the end of core collapse. There it was shown that the standard paradigm of formation in a three-body encounter between single stars was very incomplete, in the sense that the encounters which form and harden a binary often involve four or more stars. In the present paper we sharpen and clarify this new picture, showing the complete dynamical history of the first long-lived binary in a system with $N = 1024$.

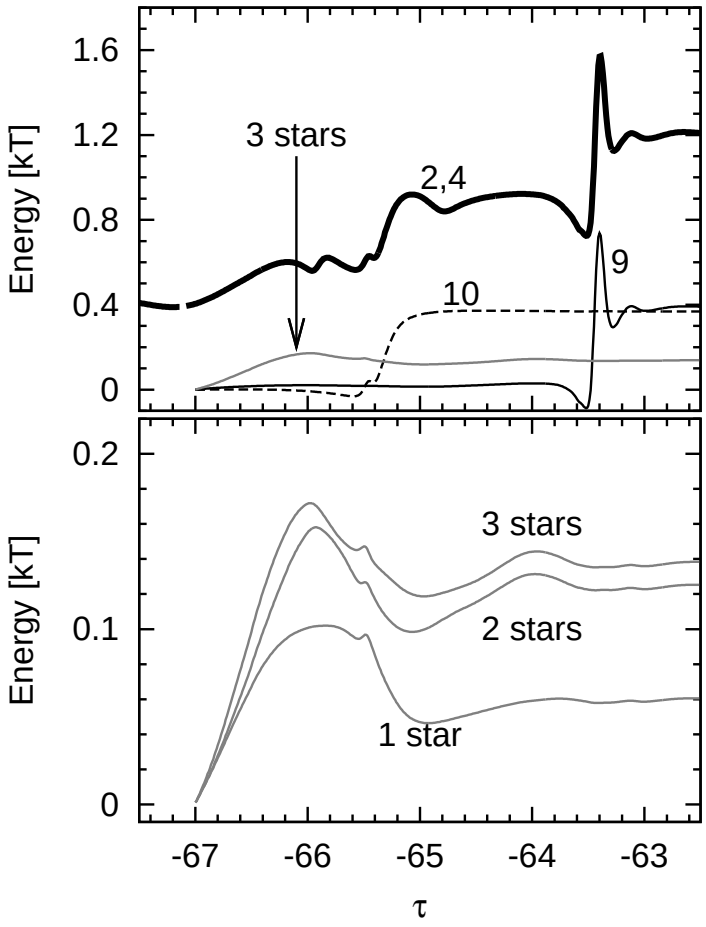

Figure 17: Time evolution of the binding energy of a pair (2,4), and of work done on the pair. In the top panel, the binding energy is indicated by the thick black curve, the work done by stars 9 and 10 by solid and dashed black curves, and the sum of work done by three stars by a solid gray curve. In the bottom panel, the work done by one, two and three of the three stars are indicated from bottom to top.

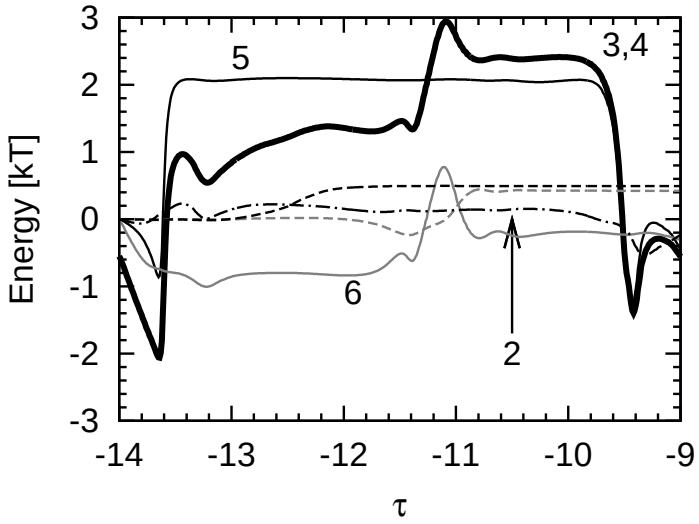

Figure 18: Time evolution of the binding energy of a pair (3,4), and of work done on the pair. Solid black and gray curves indicate work done by stars 5 and 6, respectively, the dashed-dotted black curve indicates work done by star 2, and the other curves indicate work done by two other stars.

The system we have studied is the first model from Paper I, identified there as "seed 1". The short narrative on this model in Paper I dealt with the genesis of three hard binaries, labelled there (by their components) as (1,5), (2,3) and (1,2). In the present paper we have nothing to add to what was said in Paper I on the formation of the last of these, but our more detailed analysis reveals the following phenomena:

1. In Paper I it was stated that the binary (1,5) formed in a four-body encounter, but in the present paper it has been shown (see figure 3, $\tau \simeq -1.6$) to have formed in an interaction between a bound 5-body system and an interloper which leads to (i) one escaper, (ii) the binary and (iii) three loosely-bound companions.
2. Paper I stated that the binary (2,3) emerged from a system of 5 stars, but we have now seen (see figure 3, $\tau \simeq -0.5$) that the event was an encounter between a temporarily bound three-body system and two interlopers, leading to the ejection of a soft binary from the triple system and the formation of a binary with a loosely bound companion.
3. What was described in Paper I is simply the end-game in a remarkably prolonged sequence of interactions, one of which led to the formation of a binary with a binding energy of $\simeq 9.5kT$ (where $3NkT/2$ is the initial kinetic energy of the entire N-body system). This binary did not survive, and subsequently there were periods when the maximum binding energy of any binary in the system was less than $2kT$. Nevertheless, one component of the $\simeq 9.5kT$-binary was also a component of the "final" binary.

In the following subsections we consider a number of general issues which are raised by these observations.

5.1. The role of democratic resonances

Democratic resonance is a frequent outcome of three-body interactions involving a hard binary (Hut, 1993), and leads to a triple system with a binding energy close to that of the binary.

Democratic resonances can be remarkably long-lived. Mikkola & Tanikawa (2007) found that the distribution of lifetimes (time to disruption) is approximately exponential, with an e-folding time approximately $t_{\rm d} \simeq 250$, in units where all masses are unity, $G = 1$ and the internal energy of the triple system is $E = -1$. This translates to $t_{\rm d} \simeq 250Gm^{5/2}|E|^{-3/2}$. If, as suggested above, E is close to the energy of the original binary, the virial radius of the triple

system is approximately $R = 4.5a$, where a is the semi-major axis of the binary. Assuming that gravitational focusing acts, as in the hard binary limit, we estimate the cross section for the approach of a fourth body to within a distance R to be approximately $\Sigma = 8\pi GmR/V^2$, where V is the relative speed of the fourth body and the triple system when far apart. Therefore the probability, P_4, of such a four-body encounter during the mean lifetime of the triple system is approximately

$$P_4 \simeq 9000 \times 2^{3/2}\pi n \frac{(Gm)^{1/2}a^{5/2}}{V}, \tag{5}$$

where n is the number density of single stars. The relatively large numerical coefficient is a combination of those in the expressions for $t_{\rm d}$, R and Σ, the latter two arising from the relatively large mass of the triple system.

Suppose the encounter takes place in a core with one-dimensional velocity dispersion $\sigma_{\rm c}$ and central number-density $n_{\rm c}$. Then the conventional dynamical core radius is $r_{\rm c} = 3\sigma_{\rm c}/\sqrt{4\pi G m n_{\rm c}}$, and we shall write $N_{\rm c} = 4\pi n_{\rm c} r_{\rm c}^3/3$ to represent the number of stars in the core. Approximating $n = n_{\rm c}$ and $V = \sqrt{3}\sigma_{\rm c}$ we find that the probability of a four-body encounter during the mean lifetime of a temporary three-body system is

$$P_4 \simeq \frac{2.0 \times 10^4}{N_{\rm c}^2}\left(\frac{3m\sigma_{\rm c}^2/2}{E_{\rm b}}\right)^{5/2}, \tag{6}$$

where $E_{\rm b}$, the binding energy of the binary, has been expressed in terms of the mean kinetic energy of stars in the core. Clearly, this expression has to be interpreted appropriately if it exceeds unity.

The above theory helps us to understand how typical the evolution studied in this paper is. Consider, for example, the triple system (1,5,6) which survives from $\tau \simeq -0.8$ until -0.5 (figure 3). In terms of the mean kinetic energy of all stars its binding energy is $E_{\rm b} \simeq 10 \times 3kT/2$ (the top panel of figure 13), and in terms of the mean kinetic of stars in the core the factor will be substantially less than 10. We see, therefore, that the probability of a four-body encounter during the lifetime of a temporarily bound triple system is large, even for a core with $N_{\rm c}$ as large as 10 (say). Such an example shows that the four-body behaviour seen in the system under study must occur quite frequently.

5.2. Bound few-body systems

As we have seen, it is easy to understand the formation of temporarily bound three-body systems. But the history discussed in the present paper has

examples of temporarily bound systems with larger numbers of stars. Notable examples are the five-body systems to be found in the interval $\tau \simeq -15$ to -13 and in the interval from -4.2 to -1.6, which we refer to as V_1, V_2, respectively. Each of these appears to form around a smaller existing bound subsystem. V_1 forms from the triple (6,8,9), which itself formed from the hard binary (6,9) in a democratic resonant interaction, while V_2 forms when the hard binary (3,5) captures three other single stars almost simultaneously. Roughly speaking, both of these five-body systems can be viewed as five-body analogues of a democratic resonance. In each case the binding energy of the natal binary, which acts as a kind of nucleus, leads to a temporarily bound system with five stars.

A complementary (but not contradictory) view of these five-body systems is that they represent temporary fluctuations in the size of the core. Such fluctuations are a notable feature of any N-body simulation, but their dynamical origin is little understood. The temporary capture of three single stars by a binary, which finally results in energetic ejections and in a corresponding increase of the binary's binding energy, may be one mechanism by which the core contracts to small values of the core radius. This is a rather more dynamical and active picture of extreme fluctuations of the core, compared to what is perhaps the more common understanding, i.e that fluctuations are caused by the random phases of stars as they orbit in and out of the core.

There is a sense in which the core of an N-body system is always a bound subsystem. If we compute the binding energy of that part of an isothermal model lying inside radius r, we find that its value is positive if $r > 1.58 r_{\rm c}$ approximately. In terms of star numbers, the binding energy is positive if $N > 2.22 N_{\rm c}$. In other words, if we removed the stars outside this radius, the remaining stars inside this radius would form a bound system which could not disperse to infinity as single stars. From this point of view one might think of a temporarily bound 5-body subsystem as the core of the entire system at a time when its core radius is extremely small.

In using the virial theorem, in the above discussion, we ignore pressure exerted on an imaginary sphere around the core. This pressure term is formally required in analysing the virial balance of a subset of a system (here, the cluster core) in hydrostatic equilibrium. This term, proportional to the stellar density at the surface of the imaginary sphere, is negligible compared to the density in the core. This implies that we can treat the core as a nearly isolated system, as far as the use of the virial theorem is concerned.

5.3. Immortal binaries

The conventional view of core bounce is that high densities towards the end of core collapse lead to the formation of a hard binary, which interacts with other stars to heat the core and prevent its further collapse. In the process, the binary hardens almost relentlessly, and it is usually assumed that the binary will not be destroyed (ionised) in the stream of interactions. Instead, it eventually undergoes an encounter so energetic that the binary itself is ejected, at least from the core. It is therefore perhaps a surprise to observe a binary (the pair 2,4), with energy about $9.5kT$, which appears to be essentially destroyed, leading to a period when there is no binary with an energy above $2kT$.

The probability that a hard binary is destroyed has been considered in quantitative detail by Goodman & Hut (1993), in a theoretical study based on the picture of binary formation and evolution in a uniform background of single stars. Their results (their fig. 2b) imply that a $9.5kT$ binary has a disruption probability of only about 0.5%, reinforcing the unexpected behaviour of the binary to which we have drawn attention. On the other hand we have argued that there are episodes in the subsequent evolution of this binary (and its offspring) in which the core is a compact few-body system, and in that situation the mean kinetic energy in the "core" may considerably exceed that in the entire system (which determines the value of kT). In its environment, then, the binary is not as hard as the numerical result suggests, and the probability of its disruption is much higher. Indeed Goodman & Hut (1993) show that the probability rises to 50% for a binary of energy about $2.9kT$, and so the probability of disruption in a compact core is certainly much enhanced. Clearly the limit of $10kT$, which was selected in Paper I as the end-point of the analysis, is not robust, though in the case studied here, the energy of the final binary is actually a more comfortable $16kT$.

The reason why the $9.5kT$ binary is not very hard is due to our definition of "kT". We define "kT" using the velocities of the stars at the initial time, not at the current time, and these stars are distributed throughout the whole cluster, and not only in the cluster core (see Section 2). When desired, all binding energies can be simply converted to N-body units. Our approach has the advantage that it avoids the difficulties of trying to define time-dependent or space-dependent values of kT.

Here are two examples of these difficulties, in defining 'co-moving' values of kT. First, it is not clear when or even whether to use the velocities of binary components, or only the centre-of-mass velocities, when computing

the "kT" value of a binary, when energetic binaries are present. When such binaries are relatively isolated, we could use their centre-of-mass velocities. However, in cases of strong interactions with the environment, component velocities might be more appropriate, especially during resonance interactions. Second, the value of "kT" would behave discontinuously, if we were to define "kT" strictly by velocities of stars in a cluster core, each time membership of the core changed.

5.4. Delayed Core Bounce

There remains the question of why the traditional estimates of conditions at core bounce are wrong. As discussed in Paper I, and in some more detail in Section 1 of the present paper, several treatments in the nineteen eighties showed compelling arguments for core bounce to occur when the size of the core had shrunk to contain a few dozen stars. These arguments were based on the idea that core bounce occurs when two processes are balanced: the loss of heat from the core by two-body relaxation, causing it to shrink, and the production of heat by hard binaries formed in three-body encounters. When the latter exceeds the former, core collapse can be reversed.

In these estimates, the energy generation rate is calculated by multiplying an estimate of the formation rate by an estimate of the total energy emitted by a binary while it remains inside the cluster. In reality, however, it takes time for this energy to be emitted, and it could be argued that core bounce takes place provided that a hard binary has formed and that it heats the environment fast enough. At the very least, core bounce cannot occur until the first hard binary has formed, and it is quite possible that this leads to a different condition for core bounce, one in which the number of stars in the core is smaller.

Even such an estimate for the time of formation of the first hard binary is likely to be a poor guide to the occurrence of core bounce: as we saw in the previous subsection, the emergence of an effectively immortal hard binary is surprisingly difficult. This in itself results in a delay in core bounce, which therefore takes place at a smaller core star number.

We conclude that reliable heat production from a hard binary will make itself felt only after the core has shrunk significantly further, after the point where the core traditionally was estimated to contain a few dozen stars. The arguments presented above, though qualitative, are consistent with a core dwindling to contain only half a dozen stars, as observed in the simulations presented in Paper I.

6. Conclusion

We have dissected the spacetime history of the formation of the first hard binary in a 1024-body run, in microscopic detail. This paper is the second in a series, following Paper I in which we presented the first such microscopic observation of hard binary formation during core collapse. The single run that we have investigated here in great detail is the very first run we presented in that paper. The main improvements over Paper I are:

1. We have introduced a new type of reaction diagram, somewhat similar to Feynman diagrams in perturbative quantum field theory calculations, and also similar to what was used by Hut & Bahcall (1983) in the top part of their fig. 3 (section 3.2).
2. We have introduced a new tool, in the form of work functions (section 3.1).
3. We have introduced another new tool, subcluster analysis (section 3.1).
4. We have highlighted the central role played by democratic resonances, especially three-body resonances whose longevity makes it likely that many-body interactions take place in the core of a star cluster around core bounce (section 3.7 and 5.1).
5. We have traced the network of reactions leading to the initial formation of the first hard binary back to earlier times, showing a complexity significantly larger even than what we had already unearthed in Paper I (section 4).
6. We have provided a new qualitative argument to derive the delay of core bounce, compared to standard expectations, based on the delay of hard binary heat production after formation (section 5.4).

It is interesting to note that we have employed four distinct levels of analysis:

1. *Visual analysis* of the motions of stars in the core, using an interactive visualisation tool in the form of an `open-GL` program (we have not stressed this initial phase, but it has helped to guide our intuition and to resolve ambiguities).
2. *Geometric analysis* based on pairwise distances between interacting stars.
3. *Energetic analysis* based on the binding energies of pairs and higher-order multiple stars.

4. *Dynamic analysis* based on energy transfer between tuples of stars.

These steps lead to a compressed schematic rendition in the form of the Feynman like diagram depicted in figure 3.

The next step in our explorations will be to extend the applications of our new techniques to a large number of N-body core collapse simulations, for different values of N. In order to do so, much of the analysis presented here will have to be automated. Ideally, all of the figures presented here would be generated automatically by a single analysis package. In practice, the development of such a package will remain a formidable challenge for quite a while to come.

A more modest step would be to develop improved tools to help generate many of the figures semi-automatically, requiring far less time and energy than has been the case for Paper I and the current paper, by providing better graphics tools and other diagnostic tools covering the physical properties of the core.

A next step could be to generate a kind of artificially intelligent module that is trying to guess when an interesting network of reactions starts and ends, around the time of core collapse, and whether such a network includes the formation of a surviving hard binary. Using such a tool would still require human supervision to check whether the results make sense, and to arbitrate in ambiguous situations.

Ideally, after one or more steps, we could then build a software system that fully automatically would produce all the diagrams presented in this paper for any run, including the one introduced here that resembles a Feynman diagram.

The results that we have presented could in principle be obtained from an N-body simulation code like `NBODY6`, which contains modules that allow the user to output logs with information about binaries and their hierarchy (Aarseth, 2001). An analysis of these logs are expected to produce the same result as we have obtained (for the same numerical orbits), if the user has a way to deal with the huge amount of data that would be produced. What we add here is a set of tools that enable the user to analyse those kinds of data.

We could take a further step, and add more realistic effects to our simulations, such as primordial binaries. It would be interesting to elucidate whether or not the presence of hard primordial binaries tends to suppress the formation of new binaries.

Acknowledgment

Numerical simulations have been performed with computational facilities at the Center for Computational Sciences in University of Tsukuba. This work was supported in part by the FIRST project based on the Grants-in-Aid for Specially Promoted Research by MEXT (16002003), by KAKENHI(21244020), by Yukio Hayakawa Fund, by the Netherlands Research Council NWO (grant #643.200.503), and by the Netherlands Research School for Astronomy (NOVA). Part of the work was done while the authors visited the Center for Planetary Science (CPS) in Kobe, Japan, during visits that were funded by the HPCI Strategic Program of MEXT, and Lorentz Center in Leiden, the Netherlands. We are grateful for their hospitality.

References

Aarseth, S., 2001. The Formation of Hierarchical Systems. ASP Conference Series. 228, 111–116.

Casertano, S., Hut, P., 1985. Core radius and density measurements in N-body experiments: Connections with theoretical and observational definitions. Astrophysical Journal. 298, 80–94.

Goodman, J., 1984. Homologous evolution of stellar systems after core collapse. Astrophysical Journal. 280, 298–312

Goodman, J., 1987. On gravothermal oscillations. Astrophysical Journal. 313, 576–595

Goodman, J., Hut, P., 1993. Binary-single-star scattering. V - Steady state binary distribution in a homogeneous static background of single stars. Astrophysical Journal. 403, 271–277

Hut, P., 1982, Bullentin of American Astronomical Society, 14, 902

Hut, P., 1993. Binary-single-star scattering. III - Numerical experiments for equal-mass hard binaries. Astrophysical Journal. 403, 256–270

Hut, P., Bahcall, J. N., 1983. Binary-single star scattering. I - Numerical experiments for equal masses. Astrophysical Journal. 268, 319–341

Hut, P., Inagaki, S., 1985. Globular cluster evolution with finite-size stars - Cross sections and reaction rates. Astrophysical Journal. 298, 502–520

McMillan, S. L. W., Hut, P., Makino, J., 1990. Star cluster evolution with primordial binaries. I - A comparative study. Astrophysical Journal. 362, 522–537

McMillan, S. L. W., Lightman, A. P., 1984. A Unified N-Body and Statistical Treatment of Stellar Dynamics - Part Two - Applications to Globular Cluster Cores. Astrophysical Journal. 283, 813–824

Mikkola, S., Tanikawa, K., 2007. Correlation of macroscopic instability and Lyapunov times in the general three-body problem. Monthly Notices of the Royal Astronomical Society. 379, L21–24

Spitzer, L., 1987. Dynamical Evolution of Globular Clusters, Princeton, Princeton University Press

Spitzer, L., Hart, M. H., 1971. Random Gravitational Encounters and the Evolution of Spherical Systems. I. Method. Astrophysical Journal. 164, 399–410

Tanikawa, A., Fukushige, T., 2009. Effects of Hardness of Primordial Binaries on the Evolution of Star Clusters. Publications of the Astronomical Society of Japan. 61, 721–736

Tanikawa, A., Hut, P., Makino, J., 2012. Unexpected formation modes of the first hard binary in core collapse. New Astronomy. 17, 272–280 (Paper I)